

Supplementary Information

Experimental and Theoretical Studies of the ancillary ligand (*E*)-2-((3-amino-pyridin-4-ylimino)-methyl)-4,6-diterbutylphenol in Rhenium(I) core

Alexander Carreño^{1,10*}, Manuel Gacitua², Eduardo Schott³, Ximena Zarate⁴, Juan Manuel Manriquez³, Marcelo Preite⁵, Sonia Ladeira⁶, Annie Castel⁶, Nancy Pizarro⁷, Andrés Vega^{7,8}, Ivonne Chavez⁹, Ramiro Arratia-Perez^{1,10}

¹Doctorado en Fisicoquímica Molecular, Center of Applied Nanosciences (CENAP), Universidad Andres Bello, Ave. Republica 275, Santiago, Chile, Zip Code: 8370146.

²Departamento de Química Inorgánica, Facultad de Química, Pontificia Universidad Católica de Chile. Current addres: Center of Applied Ecology and Sustainability (CAPES), Universidad Adolfo Ibáñez, Peñalolén, Chile

³Laboratorio de Bionanotecnología, Universidad Bernardo O'Higgins, General Gana 1702, Santiago, Chile.

⁴Dirección de Postgrado e Investigación, Universidad Autónoma de Chile, Av. Pedro de Valdivia 641, Santiago, Chile.

⁵Departamento de Química Orgánica, Facultad de Química, Pontificia Universidad Católica de Chile.

⁶Université Paul Sabatier, Institut de Chimie de Toulouse (FR 2599), 118 route de Narbonne, 31062 Toulouse cedex 9, France.

⁷Departamento de Ciencias Químicas, Facultad de Ciencias Exactas, Universidad Andres Bello.

⁸Centro para el Desarrollo de la Nanociencia y la Nanotecnología, CEDENNA

⁹ Departamento de Química Inorgánica, Facultad de Química, Pontificia Universidad Católica de Chile.

¹⁰Núcleo Milenio de Ingeniería Molecular para Catálisis y Biosensores, ICM

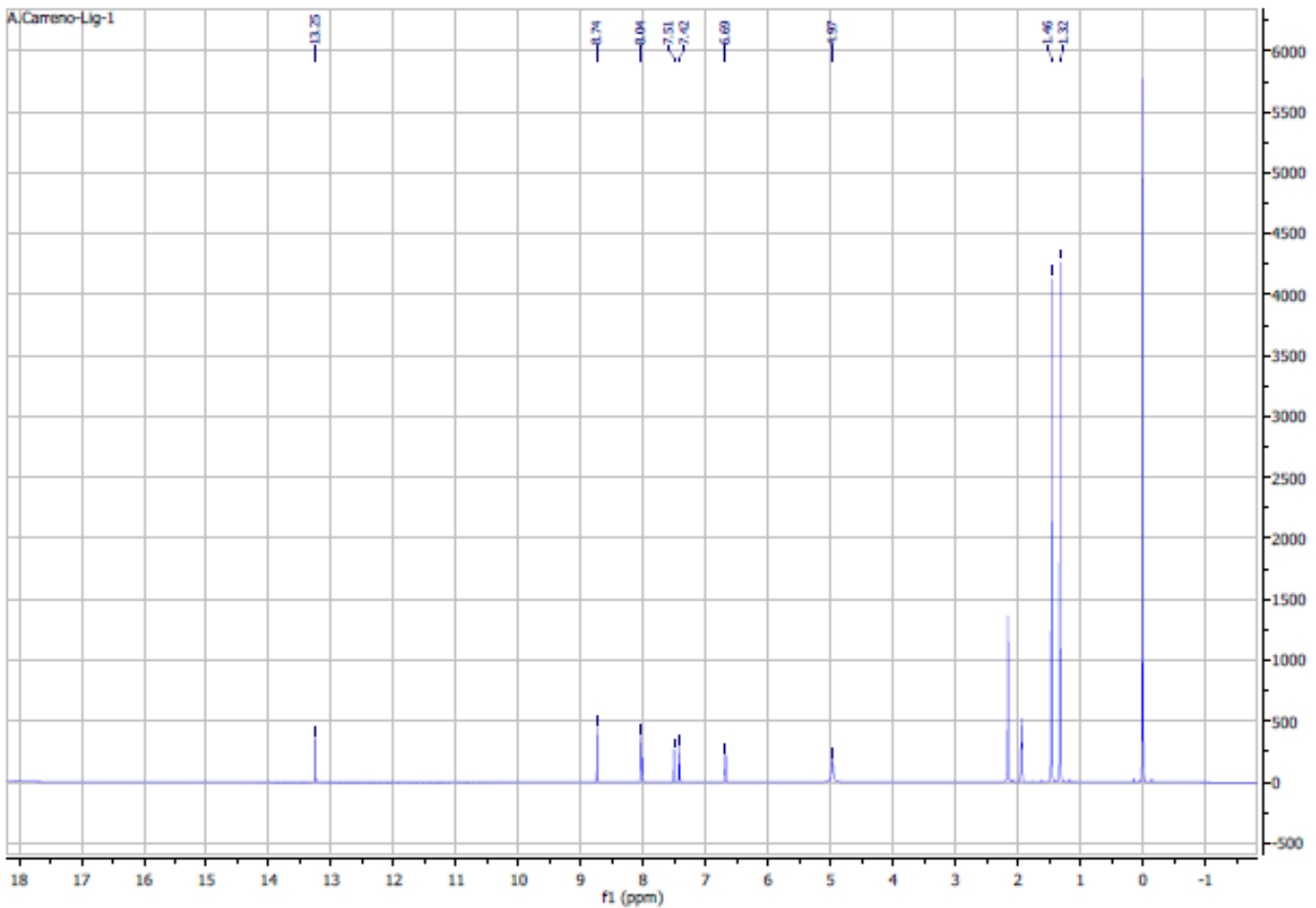


Figure S1. ^1H NMR spectra of **L** in acetonitrile deuterated.

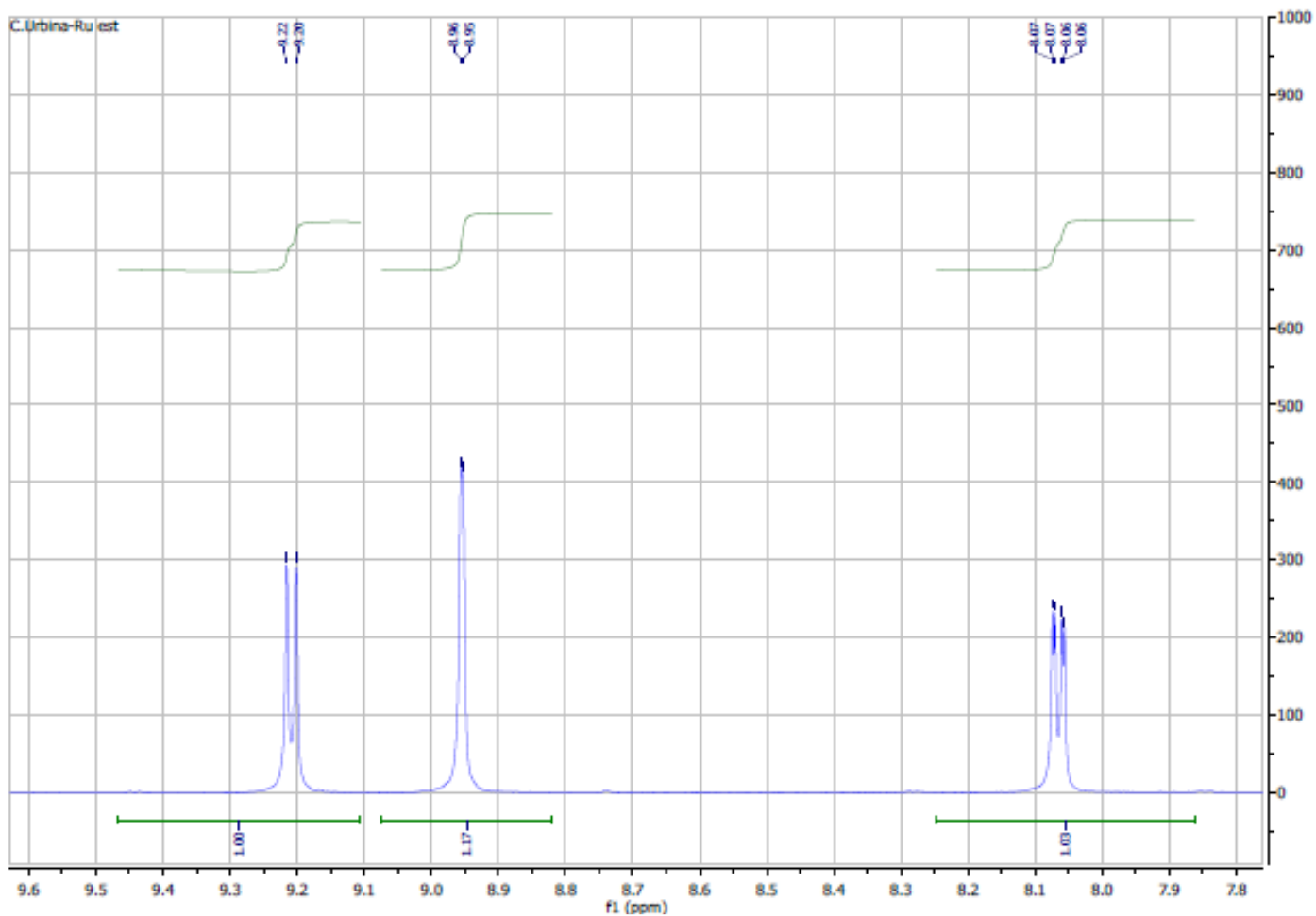


Figure S2. ^1H NMR of **C1** in acetonitrile deuterated.

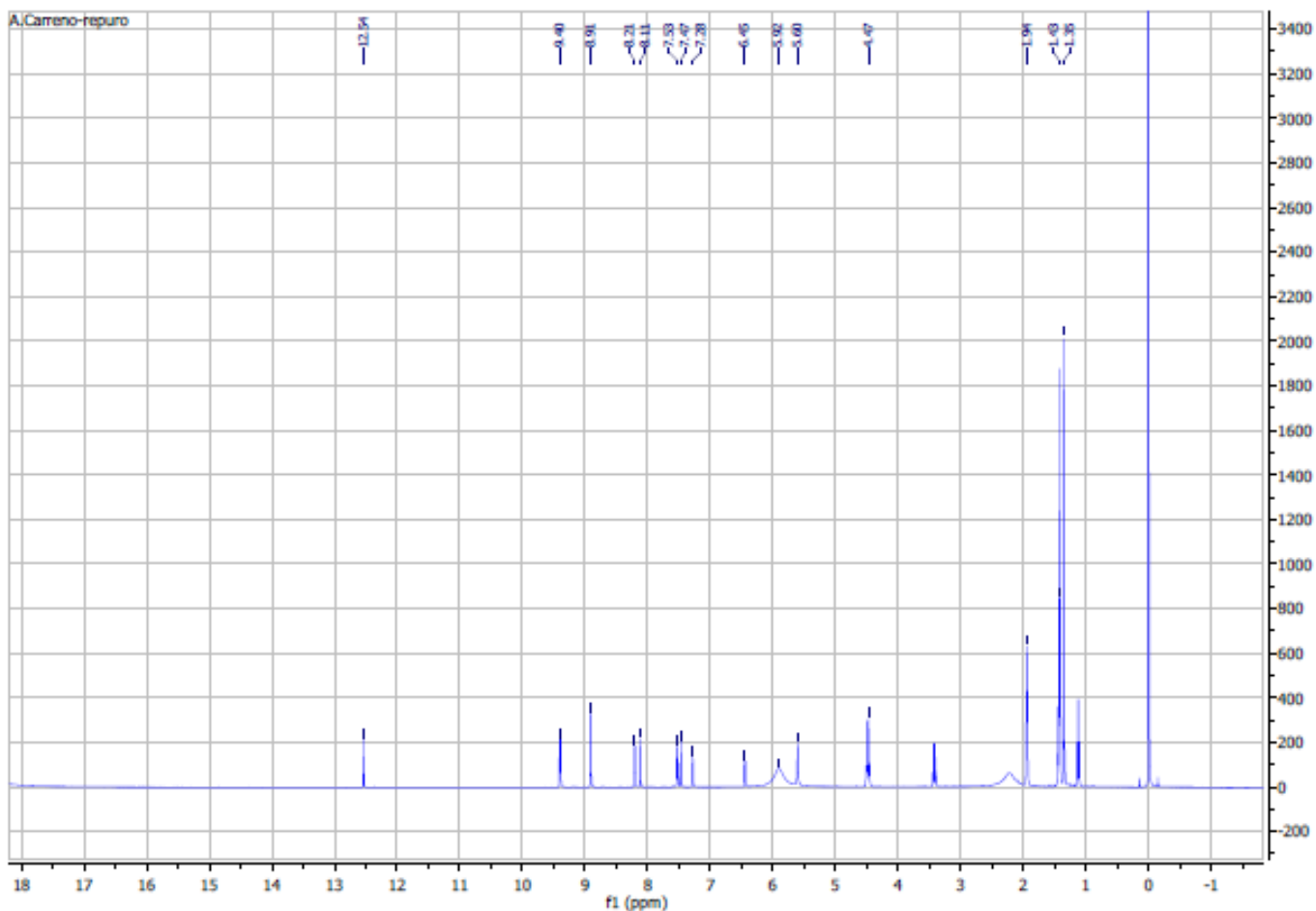


Figure S3. ¹HNMR of **C2** in acetonitrile deuterated.

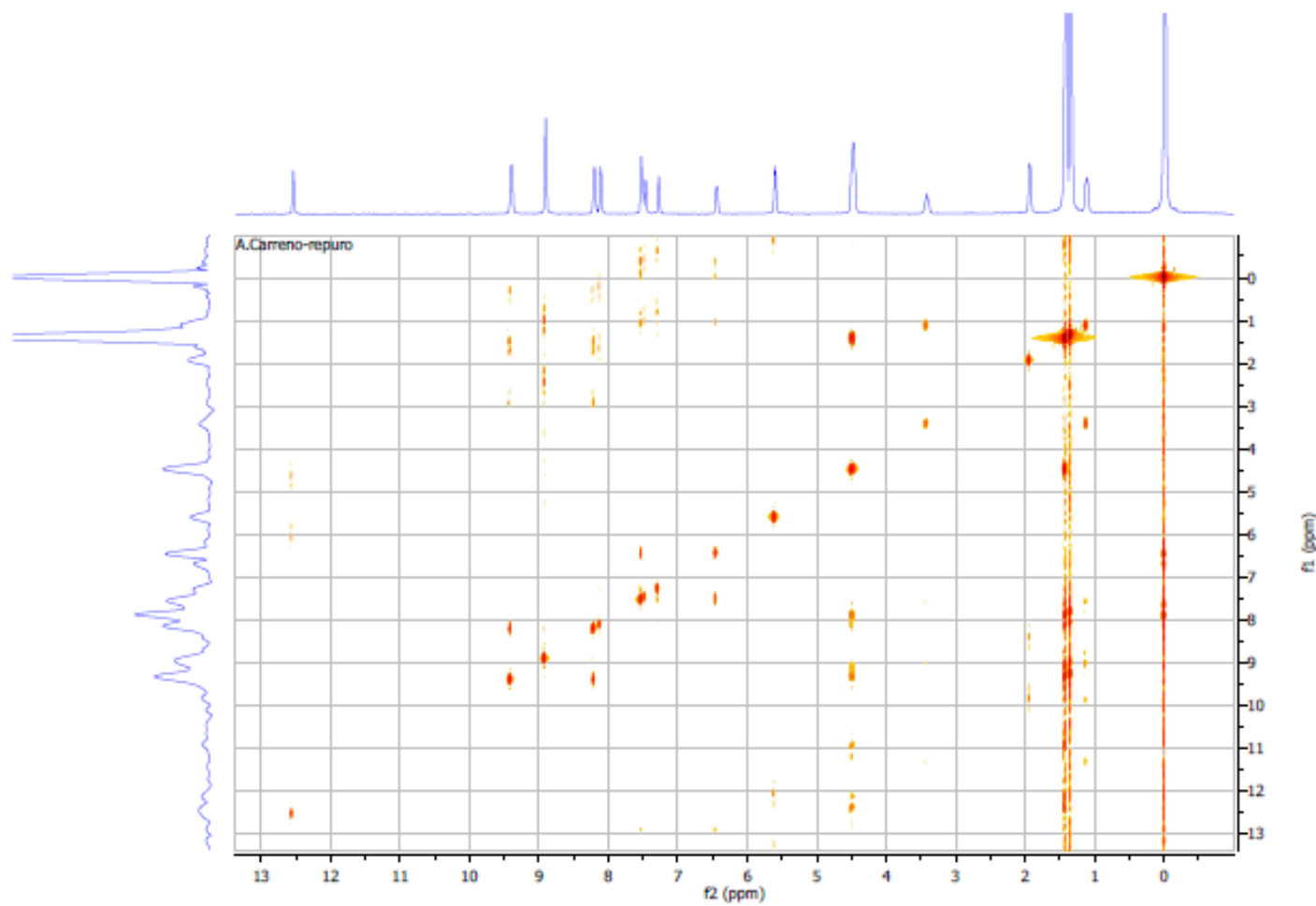


Figure S4. HHCOSY of **C2** in acetonitrile deuterated.

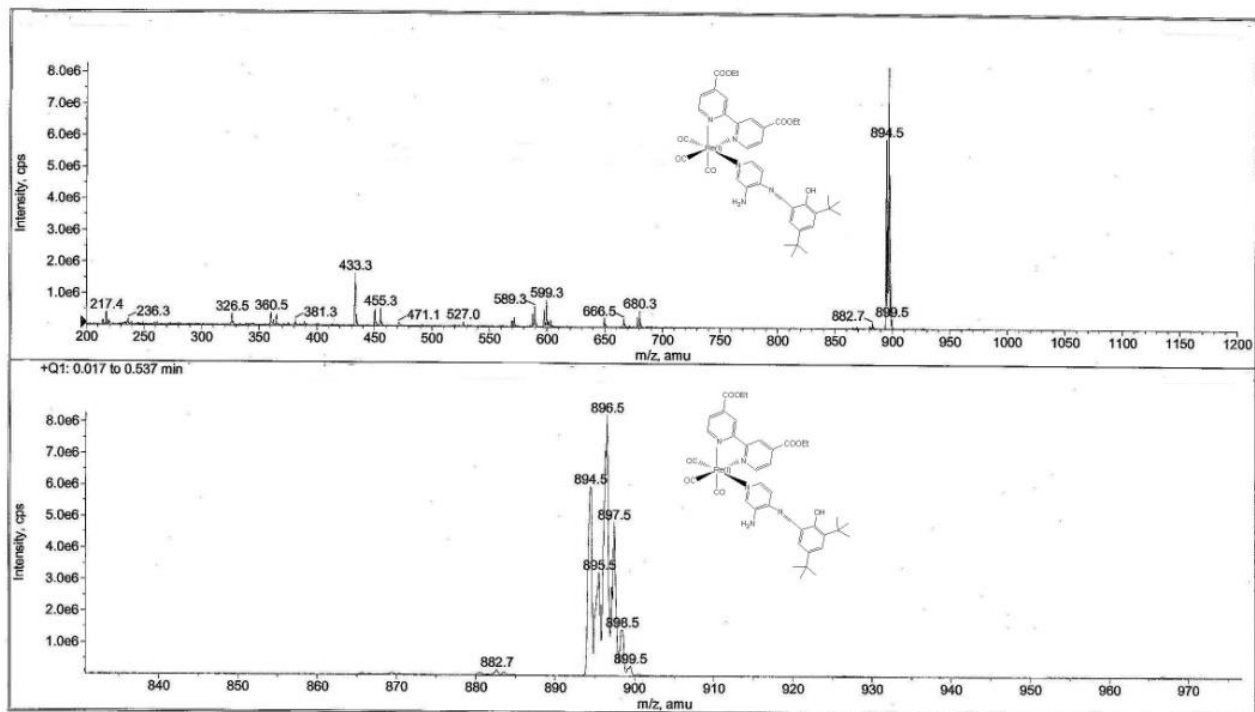


Figure S5. Mass spectra of **C2**.

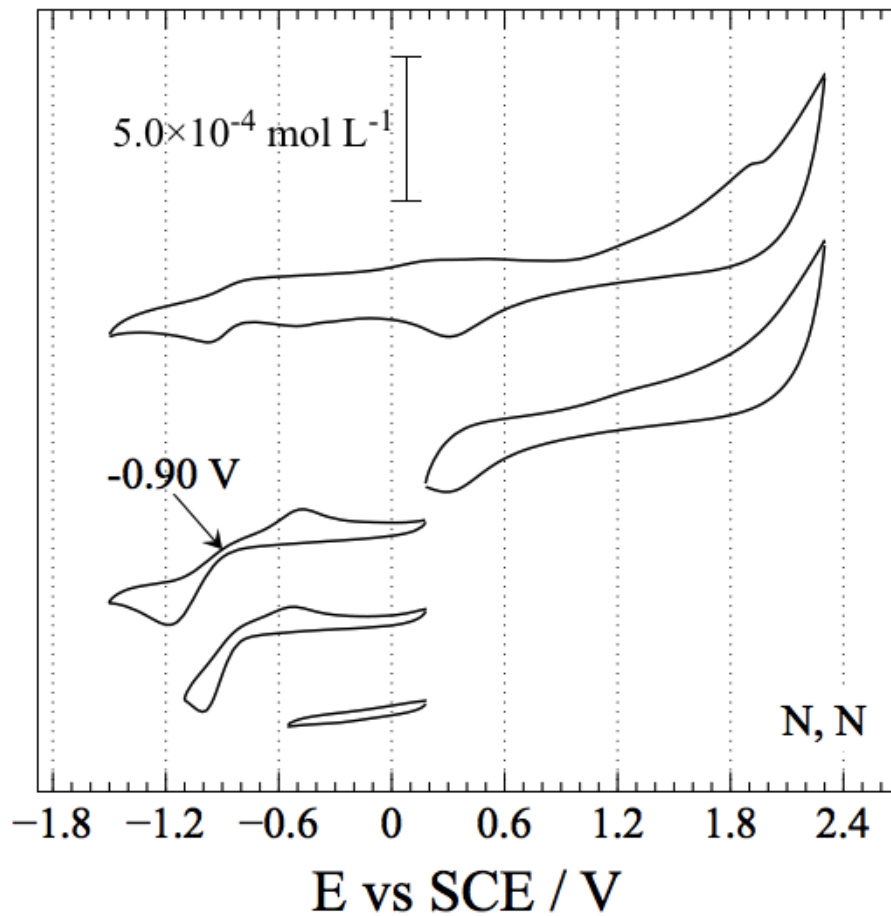


Figure S6. CV working-window study of **deeb**. Interface: Interface: Pt | 1.0 × 10⁻⁵ M of analyte + 1.0 × 10⁻⁴ M TBAPF₆ in anhydrous CH₃CN under an argon atmosphere.

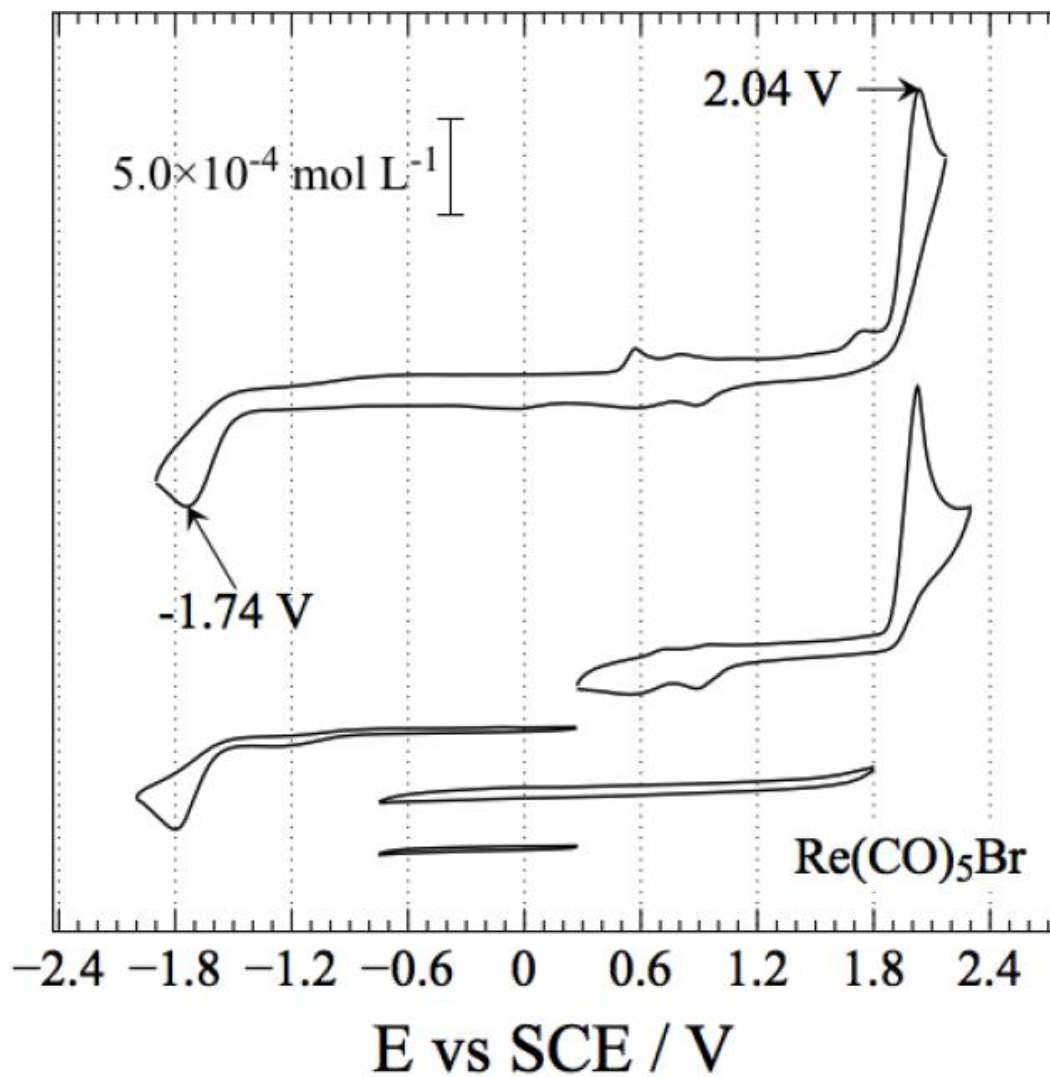


Figure S7. CV working-window study of $\text{Re}(\text{CO})_5\text{Br}$. Interface: Pt | $1.0 \times 10^{-5} \text{ M}$ of analyte + $1.0 \times 10^{-4} \text{ M}$ TBAPF₆ in anhydrous CH₃CN under an argon atmosphere.

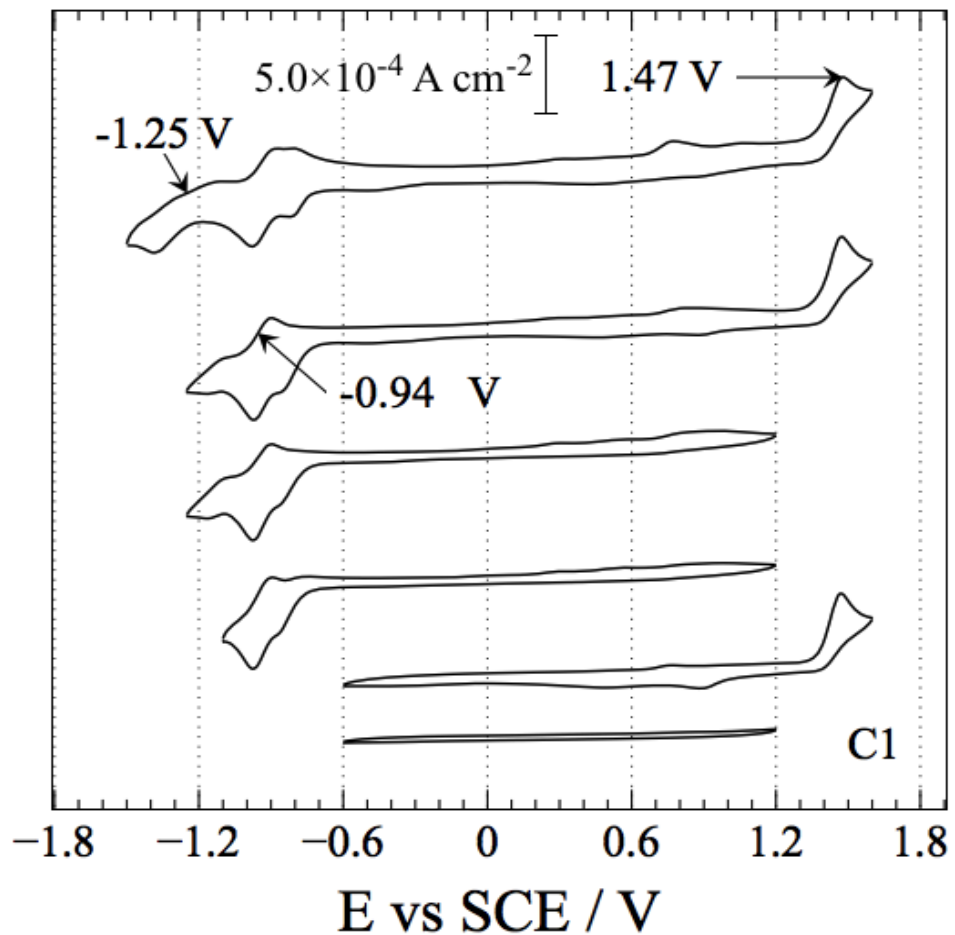


Figure S8. CV working-window study of **C1**. Interface: Pt | $1.0 \times 10^{-5} \text{ M}$ of analyte + $1.0 \times 10^{-4} \text{ M}$ TBAPF₆ in anhydrous CH₃CN under an argon atmosphere.

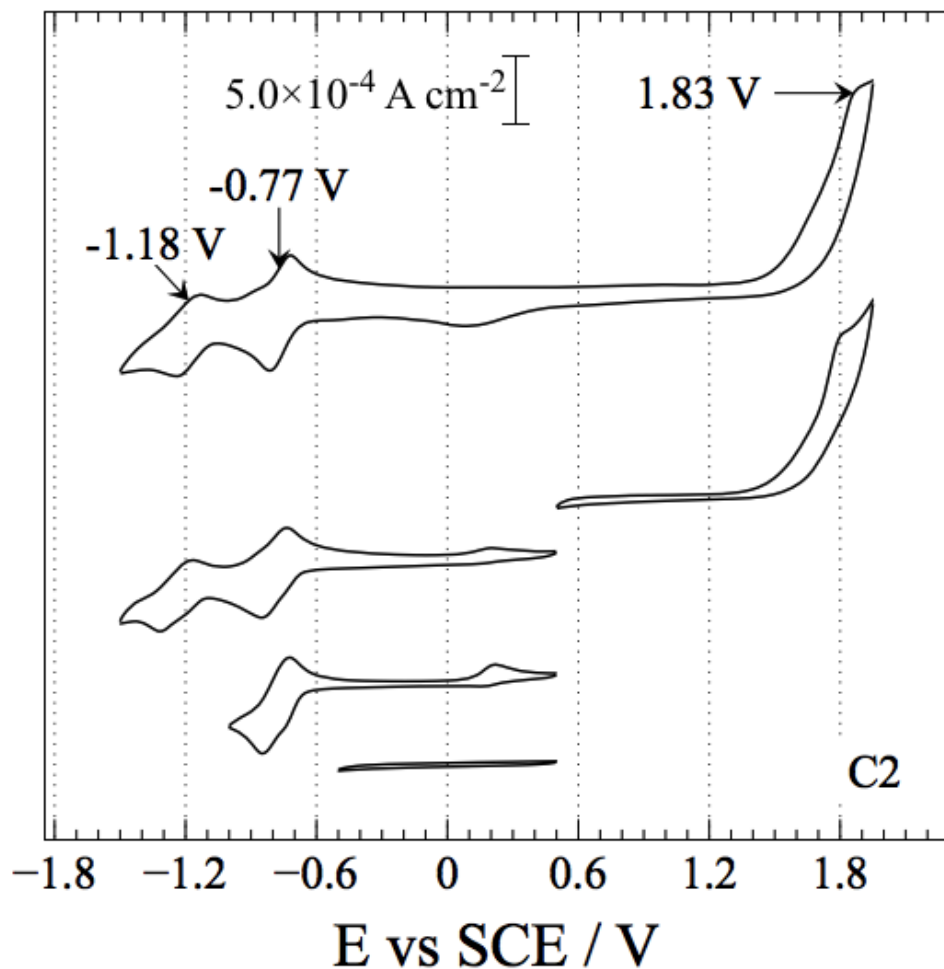


Figure S9. CV working-window study of **C2**. Interface: Pt | 1.0×10^{-5} M of analyte + 1.0×10^{-4} M TBAPF₆ in anhydrous CH₃CN under an argon atmosphere.

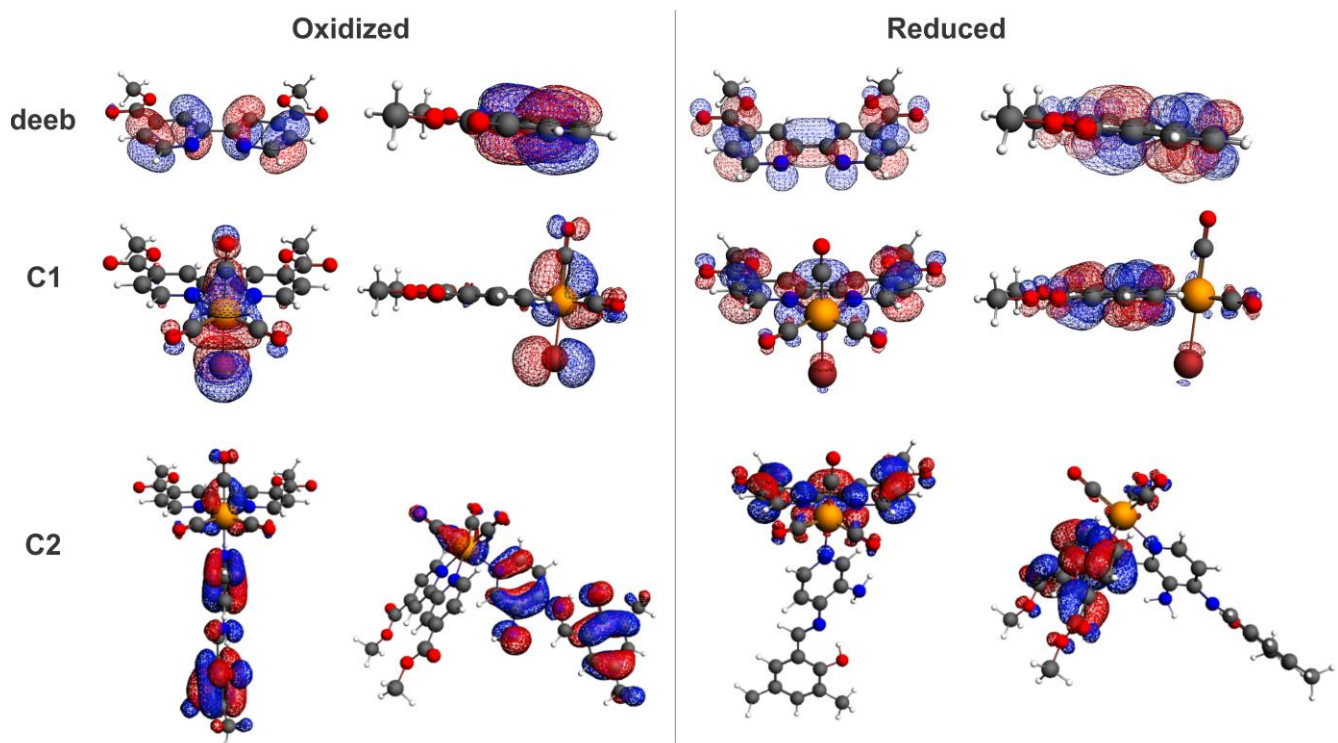


Figure S10. Two sides of view of the highest occupied orbitals of the oxidized and reduced states for deeb, C1 and C2.

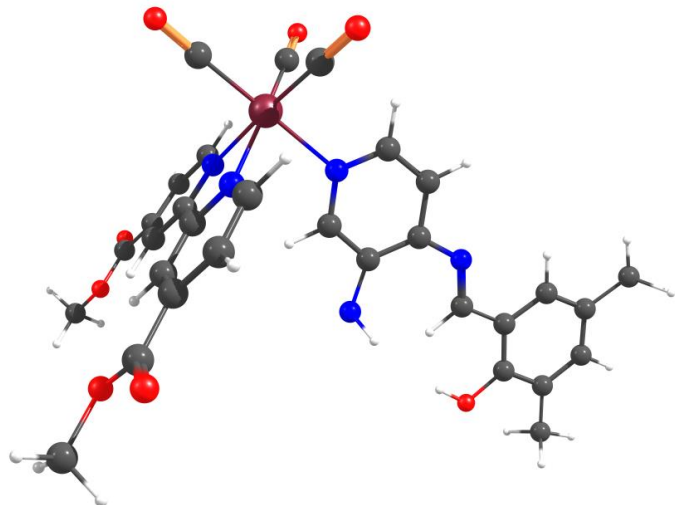


Figure S11. Optimized structure of C2 without the hydrogen bond in the L.

Table S1. Composition in percentage (%) of the frontier molecular orbitals for **C1**. The HOMO is indicated in bold.

Orb.	C≡O	Br	Re	deeb
80 γ 1/2	0	0	0	100
79 γ 1/2	0	0	0	100
78 γ 1/2	3	3	4	90
77γ1/2	37	48	11	0
76 γ 1/2	9	75	16	0
75 γ 1/2	29	9	60	2
64 γ 1/2	1	0	2	97

Table S2. Composition in percentage (%) of the frontier molecular orbitals for **C2**. The HOMO is indicated in bold.

Orb.	C≡O	L	Re	deeb
130 γ 1/2	100	0	0	0
126 γ 1/2	14	48	4	34
123 γ 1/2	1	99	0	0
121 γ 1/2	0	0	0	100
120 γ 1/2	4	0	3	94
119γ1/2	0	100	0	0
118 γ 1/2	9	88	3	0
116 γ 1/2	6	76	18	0
114 γ 1/2	30	4	65	2
111 γ 1/2	0	100	0	0